The difference between microscopic viscosity and macroscopic viscosity of crystal-bearing magmas

*Toshikazu Kawanami[1], Kazuto Saiki[1]

1.Department of Earth and Space Science,Graduate School of Science Osaka University

Magma is a mixture of silicate melts, crystals and bubbles. The amount of crystal and bubble particles in magmas significantly affects its viscosity, which increases dramatically as particle volume fraction increases. Viscosity estimation of magmas is important when we understand the time and space scales of volcanic activities, hence viscosity measurements in analogue experiments and melting experiments were actively conducted. We propose that multi-phase fluids like magmas have two different, apparent viscosities. One is defined as “microscopic viscosity”. It appears when micro objects like crystals move in a magma chamber. The other is defined as “macroscopic viscosity”. It is a bulk viscosity, and appears when a magma rises in the volcanic conduit. In previous analogue experiments for solid-liquid fluids, falling-ball viscometry [1] is considered to measure microscopic viscosity and a rotational viscometer [2] is considered to measure macroscopic viscosity. However, in previous researches, there was no experiment that compares viscosities obtained by these two different methods. Therefore, this study was performed to clarify the differences between microscopic viscosity and macroscopic viscosity by measuring viscosities of one solid-liquid fluid by falling-ball viscometry and with a rotational viscometer.
Material and Experimental Technique: Suspensions of plastic beads of two different radius (0.75mm, 1.5mm with density=930kg/m^3) immersed in corn syrup (Karo corn syrup with density=1400kg/m^3 and viscosity η~7 Pa・s at 23℃) were used as analogues of crystal-bearing magmas. We prepared ten different suspensions by changing particle radius (0.75mm,1.5mm) and particle volume fractions (F_p =0,5,10,20,30%). Microscopic viscosity was measured by falling stainless steel balls of three different radius (0.75mm with density=9620kg/m^3 , 2.5mm with density=7960kg/m^3, 4.76mm with density=7950kg/m^3) into a 100ml, φ51mm glass beaker filled with the magma analogue. Macroscopic viscosity was measured using a coaxial double cylinder rotational viscometer that is of Kawanami’s own making. We changed the voltage (1.0V, 1.5V, 3.0V) applied to the motor, to investigate the shear thinning behavior.
Results: We used the viscosities measured with a rotational viscometer driven by 1V as representative macroscopic viscosities, because the effect of shere thinning looks low enough. At R_{susp}=0.75mm, where R_{susp} is the radius of the suspended particles, the ratio of values of microscopic viscosity to those of macroscopic viscosity, $\eta_{micro}/\eta_{macro}$, were about 0.7~0.9 under the conditions that R_{fall}/R_{susp} is 1.0 or 3.3, where R_{fall} is the radius of the falling ball, and F_p is less than 20%. Moreover, it is suggested that $\eta_{micro}/\eta_{macro}$ is almost 1 under the condition that R_{fall}/R_{susp} is 6.4 and F_p is less than 30%. At R_{susp}=1.5mm, $\eta_{micro}/\eta_{macro}$ is ranging from 0.6 to 0.9 under the conditions that R_{fall}/R_{susp} is 0.5. 1.7, or 3.2 and F_p is less than 20%.
Reference
[1]Milliken WJ et al. (1989) Physicochem Hydrodynam, 11(3), 341-355.
[2]Gaudio PD et al. (2013) Geochemistry Geophysics Geosystems, 14(8), 2661-2669.

Bubble coalescence in silicate melts: mathematical formulations and experimental observations

*Atsushi Toramaru[1], Matteo Masotta[2]

1.Department of Earth and Planetary Sciences, Faculty of Sciences, Kyushu University, 2.National Institute of Geophysics and Volcanology, Rome, Italy.

Bubble coalescence deeply affects the dynamics of conduit flow during volcanic eruptions by modifying the rheology of the magma and through the development of structural heterogeneity. To model bubble coalescence in silicate melts, we present a new set of equations that describe the efficiency of the coalescence process as a function of the timescales for diffusive growth and melt-film drainage from bubble-bubble interfaces. The frequency of bubble coalescence is controlled by the timescales of these two processes, which is in turn regulated by the composition and viscosity of the silicate melt. When the vesicularity is less than half, coalescence efficiency varies as a function of the diffusivity of degassing volatiles in melts. At higher vesicularity, the coalescence efficiency is controlled by the melt film drainage. The model predicts an exponential decay of the bubble number density (BND) with time and the exponential bubble size distribution (BSD) function at stagnant conditions, and is in good agreement with in-situ experimental observations of bubble coalescence in basaltic, andesitic and rhyodacitic melt for lower vesicularities. The formulation can be used to estimate an original value of BND formed by a nucleation event using BSDs measured by the textural analysis for pyroclasts which experienced the bubble coalescence. In addition, from values of slopes of approximated BSDs, we can estimate the timescale of magma ascent or the laps time from the onset of bubble coalescence to the quenching. These textural observations for original BNDs and magma ascent timescales allow us to understand roles played by bubble coalescence in cotrolling the eruption styles and the shifts, using the combined method of geophysical monitoring and modelling.

Keywords: bubble coalescence, BND (bubble number density), BSD (bubble size distribution)

Sawtooth wave-like pressure changes (STW) appeared in a slug flow experiment: Toward understanding of volcanic oscillation systems

*Yo Kanno[1], Mie Ichihara[1]

1.The Earthquake Research Institute, the University of Tokyo

We are developing a laboratory eruption experiment system to investigate multi physics of volcano eruptions. In this study, we focus on a sawtooth wave-like pressure change (STW) observed in a preliminary system that is a syrup eruption experiment. The STW is cyclic pressure changes of which a cycle consists of a gradual pressure increasing stage and an abrupt pressure drop stage. STWs have been observed at many active volcanoes as geodetical signals including tilt, displacement [Genco and Ripepe, 2010; Ohminato et al., 1998].
An apparatus for a slug-flow experiment was designed based on the syrup eruption experiment. This apparatus was equipped with a gas chamber (volume, V_c) and a vertical pipe for a slug flow. Initially the pipe was partially filled with the syrup to the height of H_s from the end. Then, gas was injected at a constant mass flux (Q_{in}) to the chamber to flow into the pipe pushing up the syrup in the pipe. Two representative flow patterns were observed in the pipe. One was characterized by alternate layers of syrup slugs and gas slugs ascending in the pipe, which we called a slug flow. The other was characterized by repetitive transitions between the slug flow and an annular flow, which we called a slug-annular flow oscillation. The STW was observed during the slug-annular flow oscillation.
Pressure change in the chamber and acoustic waves at the vent of the pipe were measured. These measurements were assumed to correspond to geodetic and infrasonic observations at actual active volcanoes. In the experiment, the flow patterns were also constrained by image analyses. The occurrences and features of the STW in the chamber pressure were investigated with taking V_c, Q_{in}, and H_s as the experimental parameters. The results showed that the STWs were observed if there were sufficiently large V_c and Q_{in}, and that the STW changed from periodic to non-periodic cycles with increasing Q_{in}.
A mathematical model was constructed based on the experimental results of the pressure changes and the flow behaviors in the pipe. The model took account of the compressibility of the gas in the chamber, and the nonlinearity of the pressure loss in the pipe flow due to the interaction between the ascending liquid slugs and falling liquid film along the pipe wall. The dependence of the occurrence, the period, and the amplitude of the periodic STW on the experimental parameters were well explained by the model. The model has a mathematically similar aspect compared to existing models for the volcanic oscillation.
Moreover, not only the periodic STW but also the non-periodic STW was observed in this experiment. The non-periodic STW behavior has not been captured by the present model. According to the image analyses, we inferred that the non-periodic behaviors were caused by the interaction between the ascending liquid slugs and surface disturbances of the falling liquid film. From these results, we obtain an insight that irregularity of actual eruptions can be caused not only by fluctuations in ascending flow but also by influences of descending flow such as a fall back, a drain back and a magma convection of magma in the conduit.

Keywords: Volcano, Laboratory experiment, Mathematical model

A dynamical system of conduit flow with magma density change due to gas escape

*Tomofumi Kozono[1], Takehiro Koyaguchi[2]

1.Department of Geophysics, Graduate School of Science, Tohoku University, 2.Earthquake Research Institute, University of Tokyo

In lava dome eruptions, magma viscosity change due to crystallization and magma density change due to gas escape during magma ascent generate positive-feedback mechanisms in conduit flow: as magma discharge rate increases, effective magma viscosity decreases because of delay of crystallization (i.e., reduced viscous wall friction) and magma density increases because of less efficient gas escape (i.e., reduced gravitational load), leading to further increase in the discharge rate. These feedback mechanisms induce complex features of conduit flow such as a cyclic behavior and a drastic change in flow pattern. The effect of magma viscosity change on conduit flow has already been investigated in detail in previous studies based on the modeling of a dynamical system of conduit flow. On the other hand, the effect of magma density change is not well understood, although the importance of this effect has been implied from numerical results of 1-dimensional conduit flow model. In this study, we developed a model for a dynamical system of conduit flow in which magma density change due to gas escape is taken into account, and investigated the effects of the magma density change on conduit flow dynamics.

In our model, flow variables in a cylindrical conduit are spatially averaged in vertical direction, and the conduit is connected with magma chamber surrounded by elastic rocks. The model describes time-series evolutions of magma discharge rate (Q) and pressure at the magma camber (P). In the magma chamber, the time derivative of P (dP/dt) is proportional to the difference between magma influx to the chamber and magma outflux to the conduit (i.e., Q), and its proportionality constant is the parameter $C = G/V_{ch}$ where G is the rigidity of surrounding rocks and V_{ch} is the chamber volume. In the conduit flow, a momentum conservation equation describes the relationship among P, Q, the magma viscosity, and the magma density. In order to take into account the effects of the viscosity and density changes, we calculated the average magma viscosity and density in the conduit under the assumptions of a stepwise increase in the viscosity and a stepwise decrease in the density during magma ascent. The positions of these stepwise changes are determined by the timescale for crystallization (t_c) and that for gas escape (t_g), and these timescales are controlled by magma properties such as crystal growth rate and magma permeability. The developed model enables us to systematically investigate how the evolutions of P and Q depend on the parameters C, t_c, and t_g.

On the basis of our model, we can obtain the relationship between P and Q in the fixed points (referred to as P_f and Q_f) in which the time derivatives of P and Q are equal to 0. The positive-feedback mechanisms by the viscosity and density changes generate a sigmoidal shape in the curve of the P_f - Q_f relationship: the slope of the curve is positive in the low-Q and high-Q regions, whereas it is negative in the intermediate region. In this case, the time-series evolutions of P and Q (i.e., trajectory) show a cyclic behavior when the fixed point in the negative slope is unstable. A notable feature of the effect of the density change on the P_f - Q_f relationship is that the value of P_f in region of the negative slope becomes much lower than the lithostatic pressure. We found that in this case, the magma discharge rate Q reaches 0 during the cyclic behavior in the time-series evolution, which may correspond to the cessation of an eruption. Because whether Q reaches 0 or not depends on the parameters C, t_c, and t_g, we can obtain a critical condition of magmatic and geological parameters for eruption cessation using our model.

Keywords: Conduit flow, Dynamical system, Gas escape

Linking petrological and geophysical observations: A case study of the 2011 eruption of Shinmoedake volcano

*Satoshi Okumura[1], Tomofumi Kozono[2], Takehiro Koyaguchi[3], Masashi NAGAI[4]

1.Division of Earth and Planetary Materials Science, Department of Earth Science, Graduate School of Science, Tohoku University, 2.Department of Geophysics, Graduate School of Science, Tohoku University, 3.Earthquake Research Institute, The University of Tokyo, 4.National Research Institute for Earth Science and Disaster Prevention

Three sub-plinian eruptions were observed during the 2011 eruption of the Shinmoedake volcano, which were well monitored by tiltmeter, GPS, and weather radar (e.g., Shimbori and Fukui 2012; Kozono et al., 2013). To link petrological information to geophysical observations and understand the evolution of magma ascent processes during sub-plinian eruptions, we investigated pumices from these eruptions. At the Nakadake volcano, we observed deposits of the 2011 eruption and collected pumice samples. We primarily investigated gray pumice although two types of pumice (gray and white pumice) were found in the deposits, because this type of pumice reflects major eruptive magma (Tomiya et al., 2013). Two to four pumice lapilli for each subunit were polished, and bulk groundmass and matrix glass compositions were measured. The analytical results showed that the bulk groundmass composition was almost constant for all three sub-plinian eruptions, whereas the composition of the matrix glass changed systematically. Considering that the matrix glass composition reflects the degree of microlite crystallization, we obtained the variation in microlite crystallinity during the three sub-plinian eruptions. The microlite crystallinity decreased from the early stage of the first eruption to the end of the second eruption. The final eruption showed microlite crystallinity similar to that of the first sub-plinian eruption. The porosity obtained from image analyses showed good correlation with microlite crystallinity, i.e., the samples with high and low porosity had low and high microlite crystallinity, respectively.
The petrological data above indicate the following scenario. During the first sub-plinian eruption, magma experienced outgassing and microlite crystallization, resulting in the formation of relatively low porosity magma with high microlite crystallinity. The degree of outgassing decreased during the second sub-plinian eruption and the microlite crystallinity decreased. The magma erupted by the final sub-plinian eruption experienced outgassing and crystallization similar to that of the first sub-plinian eruption. The variation in microlite crystallinity can be explained by considering the change in magma decompression rate and/or the change in the final pressure at which the magma is quenched (e.g., Riker et al., 2015).
Linking the petrological and geophysical observations allows us to understand more details of temporal evolution of explosive eruptions. Geodetic data indicated that the magma fluxes were almost constant during the three sub-plinian eruptions, whereas the pressure in the magma chamber monotonically decreased corresponding to the eruptions (Kozono et al., 2013). These observations are counterintuitive because it is commonly expected that the flux decreases in response to the decrease in the pressure of the magma chamber under the assumption of magma chamber of constant volume. However, these paradoxical observations (at least those from the first and second sub-plinian eruption) may be qualitatively explained by considering that magma fragmentation pressure increased, as recorded in the groundmass of pumices, i.e., the decrease in microlite crystallinity observed from the first to the second sub-plinian eruption. According to the steady conduit flow model (Kozono and Koyaguchi, 2009; Koyaguchi, 2016), even when the magma chamber pressure decreases, the magma flux can be kept constant if the fragmentation pressure slightly increases so that the length of gas-pyroclastic flow regime in the conduit increases, i.e., the

level of the fragmentation surface descends.

Keywords: Eruption dynamics, Magma fragmentation, Petrological and geophysical observations

AD 2015 eruptive activity induced by basalt input at Sakurajima volcano: Inference from petrological monitoring data

*Akiko Matsumoto[1], Mitsuhiro Nakagawa[1], Masato Iguchi[2]

1.Graduate School of Science, Hokkaido University, 2.Disaster Prevention Research Institute, Kyoto University

Sakurajima volcano, located in southern Kyushu, Japan, has resumed its eruptive activity at Showa crater since June 2006. After that, the volcanic explosions has been continued until 2013. Although the number of explosions declined in 2014, the volcano had become higher level of eruptive activity accompanied with clear inflation since January 2015. In addition, the dyke intrusion event had occurred in August 2015. In order to reveal the magma plumbing system of the 2015 eruptive events, we carried out the petrological examination of the 2015 juvenile lapilli. We also discussed the possible reason for the activation of the 2015 eruptive activity.
The 2015 juvenile lapilli consists of lithic, scoria, pumice, and a small amount of altered rocks. Plagioclase, orthopyroxene, clinopyroxene, and Fe-Ti oxides are the dominant phenocryst phases, and a small amount of olivine phenocrysts are often occurred. The core compositions of the olivine phenocrysts without reaction rim are Fo80-81, compositionally disequilibrium with the co-existed pyroxenes. On whole-rock chemistry, the 2015 juveniles range 58.3-59.0 wt.% in SiO_2, exhibiting the most mafic compositions in all the samples since 2006. These samples are plotted on the same compositional trends of the juvenile materials since 2006 on Harker diagrams. On matrix glass chemistry, the 2015 juveniles show clearly lower in SiO_2 than those of the activity before 2014. In addition, within 2015, the silica content becomes lower with time.
The similar petrological features to the juveniles since 2006 as well as the consistency in the compositional trends of whole-rock chemistry suggest that the magma plumbing system since 2006 has been continued in 2015. The most mafic compositions of the 2015 juveniles both in whole-rock and matrix glass chemistries reflect that the considerable input of basaltic magma had occurred since 2015. Comparing to the geophysical monitoring data since January 2015, as the ratio of the basaltic magma in erupted magma increased, the volcanic edifice inflated and the eruptive activity became larger. After that, the activity changed to the magma intrusion event. It is highly probable that the activation of the 2015 eruptive activity had been induced by newly input of basaltic magma.

Keywords: Sakurajima volcano, glass chemistry, whole-rock chemistry, temporal change

Mathematical formulation of forecasting volcanic eruption sequence based on physical models and field observations

*Takehiro Koyaguchi[1], Tomofumi Kozono[2]

1.Earthquake Research Institute, The University of Tokyo, 2.Graduate School of Science, Tohoku University

During a volcanic eruption, the intensity and style of eruption generally change with time. In order to establish a method to forecast such eruption sequences, forward and inverse problems are mathematically formulated on the basis of physical models for the magma plumbing system including the conduit flow dynamics and the magma chamber processes.
The variation of eruption sequence is characterized by how magma discharge rate, Q, changes with time as a function of magma chamber pressure, P. According to the conduit flow models, the qualitative feature of the relationship between the magma discharge rate and the chamber pressure (the Q-P relationship) during explosive eruptions is controlled by the pressure at which the conduit flow changes from a bubbly flow to a gas-pyroclast flow (i.e., the fragmentation pressure). The fragmentation pressure, in turn, depends on the mechanisms of gas-escape and magma fragmentation. The Q-P relationship during non-explosive (effusive) eruptions depends on the density change due to gas-escape process and the viscosity change due to crystallization during magma ascent in the conduit. The physical model of magma chamber processes, on the other hand, suggests that the Q-P relationship is affected by the effective compressibility and volume of magma chamber. The effective compressibility of magma chamber drastically increases when the magma contains gas phase, and hence, it depends on water content and pressure of magma. Because of the coupled effects of conduit flow dynamics and magma chamber processes, the forward model of the magma plumbing system shows diverse behavior of eruption sequences (i.e., various trajectories of the Q-P relationship).
In order to forecast the eruption sequence, we must estimate the values of parameters that control the trajectories of the Q-P relationship in the above forward model. Generally, the inverse problem of the magma plumbing system is formulated as a problem to estimate the product of volume and pressure change of magma chamber and the effective compressibility of magma chamber from the field data on ground deformation around the volcano and mass of the erupted magma. The estimation of the rest of the parameters (e.g., the density and the viscosity of magma in the conduit) requires additional field observations such as petrological data of erupted magma. The numbers and kinds of parameters that can be estimated from the inverse model depend on the mathematical characteristics of the conduit flow model. For effusive eruptions where the conduit flow is approximated by a Poiseuille flow so that P and Q are proportional, a parameter expressed by the combination of viscosity, conduit length, conduit radius, chamber volume and effective compressibility of magma chamber is collectively estimated from the decay constant of Q and P during the waning stage of the eruption. For a certain type of explosive eruptions, on the other hand, the value of the fragmentation pressure can be constrained by the trajectory of the Q-P relationship observed during the waning stage of the eruption. In the presentation, we mainly discuss how the uncertainties of the parameter estimation and the forecast of eruption sequence depend on the mathematical characteristics of the conduit flow model.

Keywords: volcanic eruption sequence, physical model, magma plumbing system

Comparison between geodetic data and volcanic conduit flow models

*Takeshi Nishimura[1]

1.Department of Geophysics, Graduate School of Science, Tohoku University

Volcanic conduit flow models have been improved from many results of geologic sample analyses and laboratory experiments, and have been used for understanding the behaviors of magma flow in the conduit based on the spatio-temporal changes of pressure and velocity etc. of volcanic flow that are numerically and analytically obtained. Since the geodetic data can quantify locations and magnitude as well as shapes of the pressure sources in the volcanic edifices, analyses of geodetic data are quite useful to directly examine the volcanic flows in real volcanoes. The present study summarizes and discusses relations between geodetic data analyses and volcanic flow model, giving attentions into gas bubble growth and rising, and out-gassing during magma ascent as well as propagation of magma-fragmentation surface in the conduit during eruptions.

Keywords: Volcanic conduit flow model, geodetic data

Lava dome eruption: Sinabung (Indonesia) vs. Unzen (Japan)

*Setsuya Nakada[1]

1.Earthquake Research Institute, University of Tokyo

Processes of lava dome eruptiosn between Sinabung and Unzen volcanoes are similar to each other; they started with phreatic eruptions which advanced through phreatomagmatic eruption to magmatic eruptions. Lava collapsed-type pyroclastic flows had repeated during the growth of the lava dome and/or flow at both volcanoes. Before the appearance of the lava in the summit crater, inflation of the volcanic bodies was observed, and, during the growth of lava dome/flow, deflation of the volcanic bodies continued with the extent decreased with time. Lava effusion rates which peaked with about 6 m3/s decreased with time at the both volcanoes. Lava of Sinabung is hornblende andesite (>900 °C), while that of Unzen is hornblende-biotite dacite (<850°C). The melts are high-silica rhyolite, and their compositions were controlled by effusion rate. At Sinabung, the precursory phreatomagmatic eruptions were vulcanian and the latest stage is characterized by repetition of small vulcanian events. Lava dome extended into a lava flow as long as 3 km long. In conclusion, the lava effusion rate change controlled the pattern of lava dome growth, and the difference of melt temperature may have controlled the explosivity and the length of lava dome/flow.

Keywords: Lava dome eruption, Unzen volcano, Sinabung volcano

Understanding of caldera-forming eruption from geological and petrological approaches

*Nobuo Geshi[1]

1.Geological Survey of Japan, The National Institute of Advanced Industrial Science and Technology

Decompression process prior to caldera collapse is one of the key processes for caldera-forming eruption. In many caldera-forming pyroclastic eruptions, precursory eruption decompresses magma chamber and consequently induces the faulting and subsidence of the roof of magma chamber. The eruption of main ignimbrite follows the onset of collapse.Formation of collapse caldera indicates that the magma pressure within a magma chamber drops below the threshold for collapse. Exposing internal structure in many eroded calderas and drilling into a young collapse calderas reveals that the collapse calderas are filled with thick intracaldera ignimbrite more than 1 km in thickness. Existence of such a thick deposit inside collapse caldera strongly suggests that the caldera collapse is simultaneous with the eruption of main ignimbrite.Many large ignimbrites are preceded by smaller pyroclastic eruption. Such precursory eruption can be a large Plinian eruption, smaller ignimbrite, or combination of both. These precursory eruptions withdraw magma from magma chamber to decompress the magmatic pressure within the chamber. The decompression reached to a threshold for collapse when the end of the precursory eruption. Petrological evaluation of decompression within a magma chamber prior to the onset of collapse is crucial to understand the trigger for the main ignimbrite.

Keywords: large-scale eruption, caldera, magma

The possibility of rapid and huge magma accumulation in the crust from dynamical point of view

*Shiori Fujita[1], Hiroshi Shimizu[2]

1.Department of Earth and Planetary Sciences, Graduate School of Sciences, Kyushu University,
2.Institute of Seismology and Volcanology, Faculty of Sciences, Kyushu University

As much as 100s-1000s km^3 magma eruption in a single event (Machida & Arai, 1992) proves huge magma accumulation in the crust before eruption. Moreover, Takada (1999) indicates several times as much as erupted magma may accumulate in the crust from ratio of erupted volume to accumulated volume. Although the magma accumulation rate for caldera eruption can be calculated to be 0.001-0.01 km^3 /year on average (Salisbury et al, 2011), its accumulation process has not clearly understood yet (Jellinek & DePaolo, 2003).
Druitt et al. (2012) examined composition of some plagioclases from Santorini volcano which emitted 40-60 km^3 of magma and concluded that a few km^3 magma were added to a magma chamber in about 100 years. This rapid magma accumulation rate is about 0.01-0.1 km^3/year, ten times as large as foregoing one. This result can be crucial for volcanic eruption prediction because the accumulation may cause large scale crustal deformation. However, this petrological result has not been examined whether it also meets the dynamic constraint or not. In order to clarify this point, our study intends to estimate the maximum magma volume that the crust can accumulate in short time by using FEM (Marc Mentat). The crust is assumed as an elastic body since about 100 years is relatively short time compared with Maxwell relaxation time of the crust.
In our analysis, we inflate the magma chamber by pressuring chamber wall and compared the resulted strain around it with the ultimate strain of the crust 10^{-4}-10^{-5} (Rikitake, 1975). Our hypothesis is that two of the influential parameters involving large magma accumulation may be magma chamber shape and a magma chamber volume that has already existed before a new magma is added (hereinafter called, “primary volume”). Therefore, the calculation was carried out for spherical magma chamber and spheroid-shaped sill which have 100-2000 km^3 of primary volume, respectively. The upper depth of magma chambers are fixed at 5 km depth (Yasuda et al., 2015); that is, the central depth of these chamber are different between models. We assumed that the surface of the Earth to be free surface, the crust to be isotropic and homogeneous, $\lambda = \mu = 40$ GPa (Mogi, 1957), and ignored the gravitational effect. In addition to this numerical calculation, we also computed two analytical formulae as a reference, Mogi model (Mogi,1958) for spherical chamber and tensile fault model (Okada,1992) for sill, under the same condition. Note that these models are only applicable on the condition that primary chamber volume are very small.
As a result, maximum shear strain exponentially decreased as primary volumes increase in both types of chambers, and the maximum value was obtained at the analytical solution. Fig.a.b shows the maximum shear strain on the surface caused by an expansion of magma chamber which has 2000 km^3 of primary volume. For both models, volume increment was proportional to the maximum shear strain, while sill had smaller intercept for same volume increment. This result means that sill-shaped magma chamber has larger potential for magma accumulation than spherical chamber when same volume of magma accumulates. However, even the primary volume is as large as 2000 km^3, the strain derived from more than 1 km^3 volume increment exceeds the ultimate strain of the crust. Generally, when a strain is bigger than the ultimate strain, the crust cannot be dealt as an elastic body because the crust around magma chamber yields or causes brittle fracture; that is, we think that the discussion which considered plastic deformation or brittle fracture is necessary when we illustrate the crustal deformation in case that a few km^3 of magma accumulate in about 100 year which Druitt et

al. 2012 proposed, regardless of the difference of magma chamber shape or variety of primary volume.

Keywords: large volcanic eruption, magma accumulation, crust, strain, stress, caldera

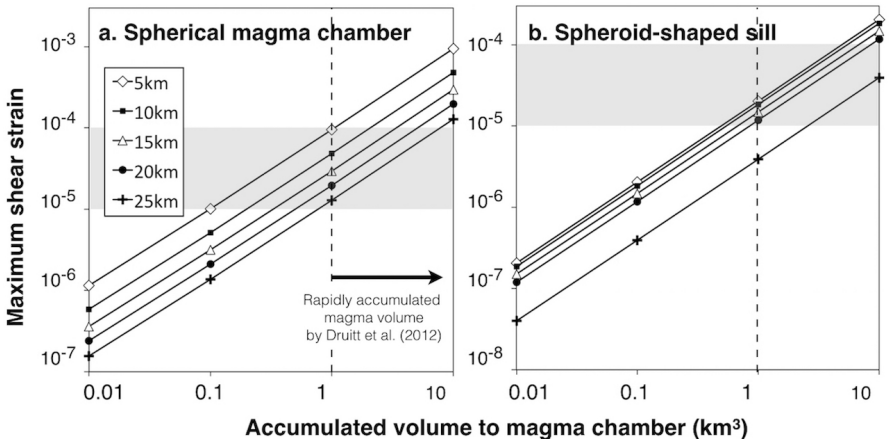

fig. a, b

The maximum shear strain in the surface versus volume increment for **a. Spherical magma chamber** (radius 7.8 km・central depth 12.8 km・upper depth 5 km) and **b. Spheroid-shaped sill** (aspect ratio 10 : 10 : 1・major radius 16.8 km・minor radius 1.68 km・central depth 6.68 km・upper depth 5 km). Primary volume is 2000 km³, respectively. The distance starts and radially directed from immediately above the chamber in the surface. The shaded region shows the probable range of the ultimate strain of the crust and the region to the right of the dash line indicates the rapid magma accumulation volume by Druitt et al. (2012).

Volcano monitor using broadcast satellite signals

*Hiroshi Takiguchi[1], Tadahiro Gotoh[1], Masatake Harada[2], Jun Amagai[1], Mikio Satomura[2]

1.Applied Electromagnetic Research Institute, National Institute of Information and Communications Technology, 2.Hot Springs Research Institute of Kanazawa Prefecture

We cannot see the change of an internal active volcano condition directly by its geography then, perceiving of its activities is difficult. To mitigate disasters by eruption, continuous volcano activity monitoring system will be desired. Most active volcanoes radiate internal thermal energy as a water vapor, and this radiation is increase with increasingly active volcano. The propagation speed of electromagnetic signal in the neutral atmosphere is delayed by the change of refractivity, which is a function its temperature, pressure, and water vapor. Therefore, to measure the propagation delay changes on volcano crater may be possible to estimate the vitalization of active volcano. We have devised a volcano activity monitor using broadcast satellite signals. In this presentation, we describe the details of the system, and show the result of feasibility survey at Hakone.

Keywords: volcano, VLBI, broadcast satellite

FEM modeling and GNSS observation around Mount Ontake volcan

*Takeo Ito[1], Kenjiro Matsuhiro[1]

1.Earthquake and Volcano Research Center, Graduate School of Environmental Studies, Nagoya University

On Septmber 27, 2014, Mount Ontake volcano was erupt. The eruption took 63 lives and represented the worst volcanic disaster in post-World War II Japanese history. Before this eruption, the GNSS observations are a few around Mount Ontake volcano. Especially, the number of GNSS observation within 4km from the summit of mount Ontake volcano is only one, which is belong to JMA. After the eruption, we establish GNSS observation network around mount Ontake volcano. New GNSS observation network around mount Ontake volcano are consistent of six continues GNSS sites. Two and four continues GNSS sites stared at 2014 and 2015, respectively. We also make seven campaign GNSS sites where are located at eastern side of mount Ontake volcano. These campaign GNSS sites are observed at July 2015.
In order to explain the observed crustal deformation, we make FEM model considering topography, such as shape of the mount Ontake volcano. In this poster, we introduce the new GNSS observation and FEM model for mount Ontake volcano.

Keywords: GNSS, Mount Ontake volcano, FEM

Characteristics of tilt changes during eruption at Sakurajima: analysis of tilt data at Amidagawa station, Japan Meteorological Agency (JMA)

*Ryosuke Nakajima[1], Takeshi Nishimura[1]

1.Department of Geophysics, Graduate School of Science,Tohoku University

Tilt change records have been used to clarify the source mechanism of volcanic eruptions and magma processes beneath the volcanoes. This study give focuses on the characteristic behaviors in temporal tilt changes during eruptions and its relations to the extrusion volume.
This study uses NS component of tilt data at Amidagawa station, which is installed 3 km away from the Syowa crater, because the data clearly records the clear tilt changes accompanied with each explosion. After eliminating tidal components in the observed tilt record using Baytap08 (Tamura et al.,2013), we selected explosive eruptions whose plume height is higher than 2000m in April and May of 2015, based on the explosion list by Kagoshima Meteorological Office. We further chose 24 eruptions in which uplift and subsidence of the crater directions are clearly observed.
In all of the events, we can see the following characteristics in tilt changes; tilt uplift rapidly toward the crater 1~2 minutes before the explosion; the uplift continues for a while, and turns to subsidence tens of seconds to a few minutes after the onset of explosion. Uplift tilt change toward the crater just after the explosion suggests that vertical upward force affect inside the conduit accompanying ash extrusion, and subsidence can be considered to represent deflation of conduit and magma chamber due to magma extrusion. Amount of tilt change of uplift, subsidence were from 2nrad to 10nrad, from 2.5nrad to 37nrad, respectively. Similarly, duration of them were from 1minute to 3.5minutes, from 10minutes to 140 minutes.
We do not see clear correlations between amount of tilt change, duration and plume height, column volume. Then, we give a focus on the amount of tilt change per unit time (tilt rate), and we find the tilt changes are classified into 2 type of subsidence; one subside rapidly within 10 minutes (Type A), and another subside gradually (Type B). Relations between tilt rate just after the start of deflation, plume height, column volume show positive correlations especially for Type A. Similar results are obtained for the uplift tilt rate.

Keywords: Tilt, Plume height, Sakurajima, Explosion

Relationship between eruption plume heights and seismic source amplitudes estimated of eruption tremors and explosion events

*azusa mori[1], Hiroyuki Kumagai[1]

1.Nagoya University Environmental Studies

It is important to analyze and interpret tremors and volcanic earthquakes for estimating eruption size and for understanding eruption phenomena. In this study, we focus on eruption tremors and explosion events to understand physical processes of eruptions and to contribute to realtime estimation of eruption size.
Previous studies investigated the relation between eruption tremor and eruption size. McNutt (2004) studied the relation between the reduced displacement (DR) of tremor and the volcano explosivity index (VEI). However, there is a wide range of DR values for each VEI, so that VEI could be overestimated or underestimated from DR. Furthermore, there are the following problems in DR: (1) The estimated DR depends on tremor's frequency, and (2) the duration of tremor is not taken into account.
Kumagai et al. (2015) estimated the source amplitudes (As) and cumulative source amplitudes (Is) for eruption tremors and explosion events at Tungurahua, Ecuador, using the amplitude source location (ASL) method based on the assumption of isotropic S-wave radiation in a high-frequency band (5-10 Hz). Their results indicated that (1) Is linearly increased with increasing As for explosion events, and (2) the log of Is was proportional to As for eruption tremors. However, the universality of these scaling relations is not confirmed yet, and the physical meanings of As and Is are also not clear.
In this study, we analyzed eruption tremors and explosion events observed at Japanese volcanoes to investigate the relations between As and Is. We used continuous seismic waveform data of Japan Meteorological Agency's volcano observation networks, which are available through the V-net website of the National Research Institute for Earth Science and Disaster Prevention (NIED). We analyzed eruption tremors and explosion events at Sakurajima (Aug. 2013-Sep.2015), Kuchinoerabu (May. 29, 2015), and Ontake (Sep. 27, 2014), for which we applied a band-pass filter of 5-10 Hz to obtain envelope waveforms. We assumed sources at vents and estimated As and Is using the ASL method. Then, we examined the relation between As and Is as well as As and the maximum heights of eruption plumes.
We obtained the linear relationship between As and Is for explosion events at the Japanese volcanoes, and these values were similar to those estimated at Tungurahua by Kumagai et al. (2015). This suggests that the linear relationship between As and Is for explosion events is universally held. Our comparison between As and maximum plume heights indicated that there is a linear relationship between them, suggesting that the plume height may be estimated from As. Is may be related to eruption volume, but it was not confirmed due to the lack of eruption volume data. Assuming the linear relationships between Is and eruption volume and between As and plume height and using the relation that the log of Is is proportional to As, we obtained the relationship that the log of eruption volume is proportional to the plume height. We compared this relation with that estimated by Mastine et al. (2009) for various eruptions in the world. We found that the proportionality coefficient between As and plume height estimated from this comparison and that estimated from the above analysis were very similar. This supports that the proportional relationship between As and plume height is widely held. However, the differences in eruption styles (vulcanian and plinian) must be taken into account in our interpretations of As and Is and their relations with the plume height and eruption volume, which are open to future studies.

The influence of the downwind on the stratigraphic GSD variation in the 2D fall and sedimentation model

*Yu Iriyama[1], Atsushi Toramaru[2]

1.Department of Earth and Planetary Sciences, Graduate School of Sciences, Kyushu University,
2.Department of Earth and Planetary Sciences, Faculty of Science, Kyushu University

The stratigraphic variation of grain-size distribution (GSD) in pyroclastic fall deposit indicates the temporal variation of GSD of settling particles, and may reflect the temporal variation of the eruption. The temporal variation of eruption, especially the temporal variation of the source GSD, affect the temporal and spatial variations of GSD in the umbrella cloud. In order to relate the stratigraphic variation of GSD to the temporal variation of source GSD, it is necessary to take into account the fractionation process from the umbrella cloud and the transportation process of ejected particles.
We developed two-dimensional fall and sedimentation (2DFS) model in order to relate the temporal variations of GSDs between the source and the sediment. Our model deals with the influence of the fractionation from an umbrella cloud and the advective transportation caused by the downwind on the sediment GSD. In this study, we assess the influence of the downwind velocity on the sediment GSD and thickness as functions of stratigraphic height and distance from the source vent by numerically calculating the analytical representation.
As a result, in the same particle size at the same distance from the source vent, the number of particles of sediment in the 2DFS model with downwind is larger than that one without downwind due to the effective shortening of fractionation times. This difference in the particle number affects the thickness of sediment. Similarly, travel time of particles, which settle at a certain distance from the source vent, with downwind is shorter than that one without downwind.
Without downwind, the order of settling particles is from the largest particles to the finer particles resulting in the normal grading structure. However, with downwind, it is possible to settle from the finer particles than the largest particles due to the dominancy of advective lateral transportation by downwind rather than by sedimentation with size sorting. This suggests that the reverse grading structure of the pyroclastic fall deposit may result from the downwind effect.

Keywords: pyroclastic fall deposit, stratigraphic variation, temporal variation of explosive eruption, effects of downwind, reverse grading structure

Changing timescale from magma mixing to ejection with eruptive timing-An example from the Shinmoe-dake 2011 eruption-

*Yuki Suzuki[1], Takeyoshi Sakai[1], Mie Ichihara[2]

1.Department of Earth Sciences, Faculty of Education and Integrated Arts of Sciences, Waseda University, 2.ERI, Univ. of Tokyo

Investigating mechanism and timescale of eruption triggering is one of the important tasks in volcanology. Injection of high temperature magma into the low temperature magma reservoir triggered the Shinmoe-dake 2011 eruption, by remobilizing the mush-like, immobile low temperature magma (Suzuki *et al.*, 2013). Some studies (Tomiya *et al.*, 2013; Suzuki *et al.*, 2013) already reported timescale from magma mixing to eruption for this eruption, by using zoning (diffusion) profiles in magnetite phenocrysts originated from the low temperature magma; that varies between 0.7h and 15.2h in Suzuki *et al.* (2013) which investigated several magnetite phenocrysts in a pumice clast erupted in the late stage of the second sub-Plinian (Jan 27AM) event. However, it remained unsolved whether timescale from magma mixing to eruption has correlation with eruption timing. If the timescale is constant throughout the 2011 eruption, it means magma mixing occurred repeatedly (e.g. Nakamura, 1995). We here focus on three sub-Plinian events (Jan 26PM, 27AM, 27PM) that occurred intermittently in the climactic phase of the 2011 eruption. To answer above question, we examined a succession of sub-Plinian deposit (Layer 2-5, Nakada *et al.*, 2013).
In this preliminary study, only Layer2-low, Layer3-low and Layer4-low (“low” means lower part of each unit) were investigated. According to Suzuki *et al.* (2014, JpGU meeting), Layer-2low and Layer-3low are from the first sub-Plinian event, and Layer-4 low is from the second sub-Plinian event. Magnetites included in ash size particles (500-1400μm) were investigated. Relatively large magnetites are preferable to read chemical and thermal history, and maximum size of magnetite phenocryst in thin sections of hand-size pumice reaches 300μm (Suzuki *et al.*, 2013). The ash particles (both pumice and free crystal) including large magnetite can be more than 500μm. The reason why we used ash size particles was to randomly pick up magnetites with various histories and mount them on single microscope slide. For EPMA analyses, we used magnetite whose rim is in contact with groundmass and whose 2D size is more than 150μm to minimize cut-section effect. To acquire zoning profiles, point analyses were carried out at 5μm intervals and 10μm intervals for marginal part (up to 20μm from rim) and inner part, respectively. Number of investigated magnetite reached ca. 20 for each eruptive unit.
Although shapes of zoning profiles have a variation for 20 crystals, all show reverse zoning in MgO. Maximum MgO contents in reversely zoned parts do no systematically change with eruptive unit, which is consistent with the continuous ejection of equally mixed magmas of the same endmember magmas (Suzuki *et al.*, 2013). We found two tendencies this time. First, most magnetites from Layer2-low have reversely zoned parts only in the marginal parts (e.g. up to 20μm from the rim), which differs from magnetites of other units. This might indicate timescale from mixing to eruption was mostly shorter in mixed magmas erupted as Layer2-low deposit. This could happen if major magma mixing occurred only in the beginning of the whole sub-Plinian activity. The second point is related to MgO contents of the unzoned inner parts. The MgO contents for 20 grains show bimodal distribution only in Layer2-low. In addition, minimum MgO contents for 20 magnetites seem lower in Layer2-low. This might show the different thermal and chemical history of the remobilized low temperature magmas depending on the stage of whole sub-Plinian activity. Additional analyses for other eruptive units (Layer2-up, Layer3-up, Layer4-up and Layer5) and calculation of absolute timescale from mixing to eruption are necessary to confirm above models.

Keywords: Eruption triggering, Shinmoe-dake, Mush-like felsic magma, Magma mixing, Magnetite, Diffusion profiles

A new technique to analyse unexposed melt inclusions in quartz

*Shumpei Yoshimura[1], Mitsuhiro Nakagawa[1]

1.Department of Earth and Planetary Sciences, Hokkaido University

We are trying to develop a new technique to analyse the volatile concentration of quartz-hosted rhyolitic melt inclusions using a micro-FTIR spectrometer without exposing the inclusions to the surface of a doubly-polished thin section. This method is similar to that of Nichols and Wysoczanski (2007) who established a technique to analyse unexposed basaltic melt inclusions in olivine phenocryst. We show the results of the feasibility examination of this technique as summarised below.
When an infrared beam transmits through both the quartz crystal and melt, the resultant spectrum (f) is considered to be the linear combination of the pure spectrum of quartz and melt: f=d(qz)*f(qz)+d(mi)*f(mi). Here, f(qz) and f(mi) represent the pure spectrum of quartz and melt per unit thickness, respectively. d(qz) and d(mi) are the effective thickness. d(qz) is calculated based on the absorbance of a quartz peak in the sample spectrum that is considered to be linearly proportional to the thickness. d(mi) is then obtained by subtracting d(qz) from the total thickness (d). Finally, the volatile concentration is estimated from d(mi) and absorbance of the volatile peaks.
The feasibility of this analytical method was examined as follows. Firstly, we analysed quartz thin sections with a micro-FTIR spectrometer to confirm that absorbance of quartz peaks, which exist in the range of 1500-2200 cm-1, is proportional to quartz thickness. The 1790 cm-1 peak was chosen as an indicator of d(qz), because this peak is free from interference with other peaks.
Secondly, we examined if the mixed spectrum of quartz and melt is the linear combination of pure spectrum of each material, by putting a thin section of obsidian on the section of quartz. We confirmed that the mixed spectrum was the linear combination, and the water content of obsidian was always calculated to a single value irrespective of the quartz/melt ratio.
Thirdly, we applied the method to a quartz-hosted melt inclusion from the Onikobe caldera super eruption. A large inclusion with 150 μm diameter was chosen for this purpose. The water content of this inclusion was determined to be 4.4 wt% by an FTIR analysis with a 10 μm beam. The same inclusion was then analysed with a thick beam with various diameter(<300μm). We observed that the resultant spectrum was not a linear combination: the water content was strongly dependent on the quartz/melt ratio. For example, the water content was calculated to be 2.3 wt% based on 3550 cm^{-1} peak when d(qz)/d =0.23. For the 4500 and 5250 cm^{-1} peaks, the water content was calculated to be 63 and 84 % of the true water content. We are now investigating why such a non-ideal behaviour was observed in melt inclusion analysis, though ideal linearity was confirmed in the quartz+obsidian superimposed sample.

Keywords: melt inclusion, quartz, FTIR

Laboratory experiments on the whole process of magma chamber solidification

*Daichi Takahashi[1], Ikuro Sumita[1]

1.Graduate school of Natural Science and Technology, Kanazawa University

How does the initially totally molten and thermally convecting magma chamber solidify ? How is the solidification process and solidification texture related ? There have been experimental (e.g., Brandeis & Marsh, *Nature*, 1989) and theoretical (e.g., Worster et al., *EPSL*, 1990) studies focusing on how the melt solidifies when it is cooled. These studies have showed a complex coupling between solidification and thermal, compositional convection, but detailed study on the whole process of solidification is still limited. Here we conduct laboratory experiments using a wax to model magma and study the whole process until complete solidification under different thermal boundary conditions.
We use a thin acrylic tank with a height 80 mm, width 80 mm and a thickness of 10 mm. We fill the tank with a wax (PEG 1000) which solidifies at 37 degrees C. We heat the tank from below using a heater at a temperature of 70 degrees C. The wax melts and thermal convection occurs. The Prandtl number of the liquid PEG is Pr = 700 and the Rayleigh number of thermal convection is $Ra=2.4\times10^{7}$. After a steady state convection is achieved, we turn off the heater and the wax solidifies. We record the cooling process using time-lapse photos and measure the temperature within the liquid and at the boundaries. We conducted experiments under the following 3 thermal boundary conditions : Case A (Cooled from above at a room temperature and insulated from below), Case B (Cooled from above by an ice water and insulated from below), Case C (Cooled from below at a room temperature and insulated from above). From these experiments, we find the following: (i) the time needed for the total solidification is the same for the 3 cases within 5 %, (ii) for cases A and B, convective pattern changed during cooling and transformed to a single upwelling at the center and two downwellings at the sides whereas for Case B, convective pattern remained unchanged during solidification and only changed immediately before total solidification, (iii) solidification texturing occurred with a pattern corresponding to the temperature field of the thermal convection immediately before the total solidification.
Our experimental results can be interpreted as follows. (i) In our experiments the time required for total solidification is comparable regardless of the thermal boundary condition. When the boundary temperature is low, solidification occurs earlier, but suppresses the heat transfer thereafter due to the thickening thermal boundary layer. This seems to be the reason for the comparable total solidification time. (ii) In our experiments, in Case B, solidification started within a time scale shorter than the turnover time and the convection pattern remained unchanged. This is consistent with the estimate that at least a convective turnover time is needed for a convection pattern to change. (iii) Our experiments show solidification texturing corresponding to the temperature field of thermal convection immediately before solidification. The thermal diffusion time for the temperature field originating from thermal convection to become homogenized can be estimated as 4 hours, assuming a convection cell size of 4 cm. On the other hand, the time needed for total solidification after the convection stops is only about 15-18 min, which is much shorter than the thermal diffusion time, which explains why solidification texturing occurred. Our experiments suggest that similar phenomena may occur in magma chambers if the same conditions describe above are satisfied.

Keywords: magma chamber, solidification process, thermal convection, solidification texturing

Rheological experiments of polyurethane foam toward simulating tube pumice

*Masatoshi Ohashi[1], Mie Ichihara[1], Atsushi Toramaru[2], Osamu Kuwano[3]

1.The Earthquake Research Institute, the University of Tokyo, 2.Department of Earth and Planetary Sciences, Faculty of Sciences, 33 Kyushu University, 3.Japan Agency for Marine-Earth Science and Technology

Tube pumice is a common product of explosive silicic eruptions forming calderas. It is characterized by bubbles which elongate in one direction. Such bubble deformation is considered to occur in the processes of magma ascending in a conduit, which include vesiculation, flow, and fragmentation. It is expected that tube pumice has recorded information about some processes leading to a caldera eruption. In the preliminary experiment, we decompressed and inflated polyurethane foam (Ohashi et al., 2015, VSJ meeting). Polyurethane foam is a candidate of analogue materials to be used to simulate the formation processes of pumice because it undergoes vesiculation, flow, and solidification at ordinary temperature and pressure. Reproducing the tube pumice structure with polyurethane foam may help discovering the key factors to produce tube pumice. Here we present the time-dependent rheological properties of the polyurethane foam, which is specifically blended for our experiment.
Material : Polyurethane foam is a polymeric solid with a cellular structure. It is produced by mixing two polymeric liquids (polyisocyanate and polyol) with a catalyst and a foam stabilizer. Including a foam stabilizer prevents bubbles from coalescing and produces a homogeneous cellular structure by stabilizing their interfaces. To avoid such a structure, we use specifically blended polyurethane foam without the foam stabilizer in this study. This polyurethane foam has elliptical bubbles, which are larger than the usual one because of coalescing.
Apparatus and Procedure : We examine the temporal change of the rheology of the polyurethane foam from inflation to solidification. A rheometer (AR2000ex) is used with a concentric cylinder. The outer cylindrical cup is made of transparent polypropylene (inner φ=23 mm) and the rotating spindle is made of aluminum (outer φ=15 mm). An infrared thermometer is mounted at the side of the cup to record its temperature. The torque and the angle of the rotation are recorded by the rheometer and the growing height of the sample is measured in the video images. The data are used to calculate the stress and strain. In oscillatory tests, the amplitude ratio and the phase difference of the stress and the strain provide us with the storage modulus (G') representing elasticity and the loss modulus (G'') representing viscosity. We conduct three experiments. First, the temporal changes of G' and G'' are examined under oscillatory rotation with the frequency of 3.16 Hz and the strain amplitude of 0.1 %. Second, the frequency dependence is assessed by changing the frequency in a measuring cycle. Finally, a large strain is applied up to 10 at the strain rate of 0.2 (s^-1) while the material is solidifying. We look into the pore structure of the representative samples with X-ray tomographic imaging (inspeXio SMX-225CT, Shimadzu Co.).
Result and Discussion : In the initial stage G'' is larger than G' indicating the material is fluid. The torque gradually increases with the gelation, so that G' is equal to G'' in 20 minutes. After that, G'' decreases and G' converges into the constant value of $10^{6.3}$ Pa. It is known that the shear modulus of magma is about 10 GPa regardless of its temperature and composition (Dingwell and Webb, 1989). We find the shear modulus of the polyurethane foam used in this experiment is lower than that of magma by four orders. In the second experiment the crossing time when G' is equal to G'' is delayed as the frequency decreases. The inverse of the angular frequency at the crossing time is regarded as the instantaneous relaxation time. This result shows the relaxation time of the material gradually increases and the time scale in which the material transits from solid to liquid

is quantified. Finally the X-ray tomographic imaging reveals that the sample of the third experiment with a large strain has elongated bubbles like tubes.

Keywords: Polyurethane foam, Tube pumice, Rheology, X-ray tomographic imaging

Mechanism of fragmentation of vesicular magma with non-uniform distribution of bubbles

*Shogo Maruyama[1], Yamato Aoki[1], Noriaki Kurokawa[1], Hiroshi Yoshida[1], Masaharu Kameda[1], Mie Ichihara[2], Satoshi Okumura[3], Kentarou Uesugi[4]

1.Mech. Systems Eng.,TUAT, 2.ERI, Univ. of Tokyo, 3.Earth Sci., Tohoku Univ, 4.JASRI

Brittle fragmentation is a key process in explosive eruption. Estimation of the decompression time in real explosive events indicates that the style of fragmentation is to be “brittle-like fragmentation” (Kameda et al., JVGR 2013), which was defined as the solid-like fracture of the material whose bulk rheological properties was close to fluid state. In this presentation, we clearly show the internal non-uniform structure of bubbles which is a major source of crack development that may lead to brittle-like fragmentation. This scenario was proposed based on our previous experiments (Kameda et al., JGUM 2014).

We used syrup containing bubbles as material of specimen because syrup has large rigidity close to magma, and can have wide range of viscosity like magma. The rapid decompression apparatus was used to simulate the fragmentation. It consisted of a pressure container whose top was sealed by a plastic film. First we compressed the specimen placed in the container by nitrogen gas. Second we heated electrically the nichrome wire adhered on the film. The rapid decompression was caused by the rupture of the film due to the heat of nichrome wire.

The specimen was hemisphere whose size was about 20 mm in diameter and 10 mm in height. The viscosity of each specimen was chosen from three values (10, 50, and 100 MPa · s) and the void fraction before the decompressionφ_0 was varied from 4% to 40%. The initial pressure just before the decompression was 2 MPa, and the characteristic time of decompression was about 3 ms.

To observe the internal structure of specimen, we conducted X-ray CT imaging at SPring-8. We took the radiograph images with the resolution of 15.5 μm/pixel. The CT imaging was conducted three times (after and before the compression and after the decompression). We observed the dynamic behavior of specimen during decompression by radiography using the same optical setup as the CT imaging. We simultaneously observed it by high speed imaging using a visible light source. We reconstructed the volumetric 3D model of the specimen based on the CBP method.

A typical example of fragmentation captured by high speed imaging is shown in Fig. 1. This experiment was conducted under η=50 MPa · s,φ_0=7.6 %. As shown in Fig. 1, the partial fragmentation occurred at 2.1 ms after the decompression was started. Reconstructed 3D image of the specimen is shown Fig. 2. As shown in Fig. 2, the specimen contains a large bubble with a small satellite bubble close to the large one (green broken line). These two bubbles are triggers of the fragmentation shown in Fig. 1. We also observed all the specimen fragmented into pieces even if its viscosity was the same as that shown in Fig. 1. Therefore, it is concluded that whether to fragment or not depends on the bubble distribution.

Next, we conducted finite element analysis of the specimen under the rapid decompression. The COMSOL Multiphysics ver. 5.0 was used as calculation platform. In order to reduce computational cost, we used a simplified 3D model of the specimen in the experiment (Fig. 2). In the model, we extracted just around the primary large bubble with a satellite small bubble. The specimen was assumed to be a Maxwell fluid whose physical properties were equal to those of syrup measured in previous study.

As shown in the result (Fig. 3), the maximum stress occurred between the two bubbles. Preliminary result (Kurokawa et al. JGUM 2015) shows that the stress concentration occurs on the surface of satellite bubble, and it leads to the increase of brittleness (Ichihara et al. JGR 2010) at the time when the stress reaches the critical value of fracture. Compared the calculation result of

surface stress field with the surface crack distribution captured by high speed photography, we found that the surface crack propagates along the line of large stress concentration. This fact indicates that we can predict the brittle fracture.

Keywords: Magma, Fragmentation, X-ray CT, FEA

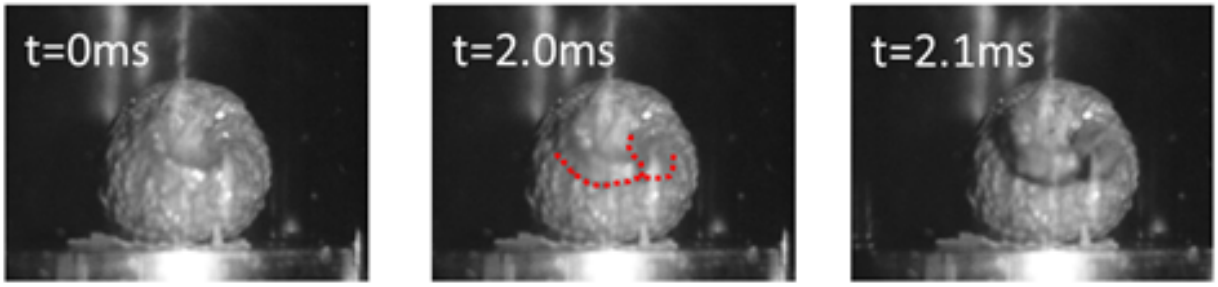

Fig.1 High-speed video images of fragmentation

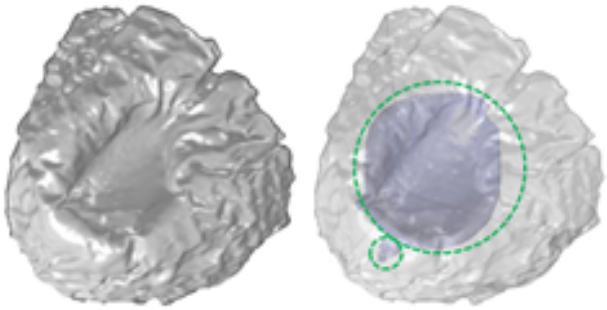

Fig.2 Surface and primary pores

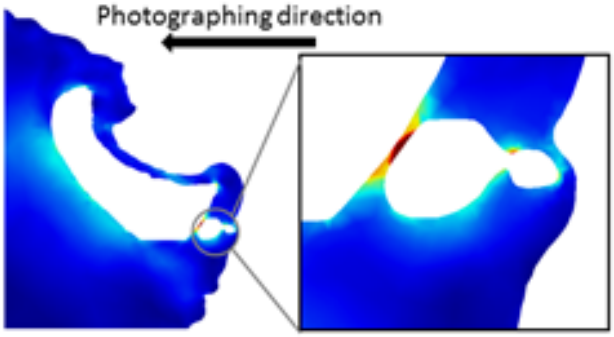

Fig.3 Stress at primary pores

